# Transmission Hardening Planning Against Extreme Weather Events Considering Cyber-Physical Interdependence

Haitao Xu
*Department of Electrical Engineering*
*Tsinghua University*
Beijing, China
xuht24@mails.tsinghua.edu.cn

Haotian Zhao
*Department of Electrical Engineering*
*Tsinghua University*
Beijing, China
zhaohaotian@tsinghua.edu.cn

Hongbin Sun
*Department of Electrical Engineering*
*Tsinghua University*
Beijing, China
shb@tsinghua.edu.cn

Qinglai Guo
*Department of Electrical Engineering*
*Tsinghua University*
Beijing, China
guoqinglai@tsinghua.edu.cn

***Abstract*—Reinforcing transmission lines prior to extreme weather events is an important measure for enhancing power system resilience. Modern power systems are cyber-physical systems (CPS) characterized by tight coupling of energy and information sides. Extreme weather can simultaneously attack both sides, making it essential to account for cyber-side impacts in transmission hardening planning (THP). This paper proposes a THP methodology that considers cyber-physical interdependence. A defender-attacker-defender (D-A-D) framework is established, which explicitly models the cyber-physical interactions. This D-A-D framework involves decision-dependent uncertainty (DDU). By exploiting the special structure of the model, the DDU is eliminated, and a solution algorithm based on column-and-constraint generation (C&CG) is developed. Case studies on modified IEEE 30-bus and 118-bus systems validate the effectiveness of the proposed model and the efficiency of the algorithm.**

***Keywords—transmission hardening planning, power system resilience, cyber-physical system, defender-attacker-defender model***

## I. Introduction

With the development of smart grids, modern power systems have evolved into typical cyber-physical systems (CPS) [1]. Control systems such as energy management system (EMS) and supervisory control and data acquisition (SCADA) have become indispensable components across all sectors of the electricity value chain, including generation, transmission, and consumption. However, the deep coupling between the cyber and physical sides has rendered power CPS more susceptible to the impacts of extreme weather events (e.g. typhoons, storms, ice disasters).

The coupling between the physical and cyber sides occurs primarily in terms of topology and functionality. Topologically, optical fiber composite overhead ground wires (OPGW) are widely adopted in China's high-voltage transmission lines, enabling the co-transmission of electrical power and critical control information. Consequently, faults such as tower collapse and line breakage caused by extreme weather events can lead to coupled cyber-physical failures. Functionally, the information flow in the secondary system governs the energy flow in the primary system, while the operation of secondary system itself depends on the energy supplied by the primary system. Any anomaly or failure in either side can significantly impact the operational state of the other, potentially triggering cascading failures [2].

There have been multiple historical cases in China where extreme weather led to cyber-physical coupling failures in the power system. For example, the rare ice-snow disaster in 2008 and Typhoon Meranti in 2016 caused large-scale contingencies of OPGW, resulting in extensive blackouts.

From the perspective of extreme weather, the concept of power system resilience has garnered widespread attention [3]. In preventive scheduling, reinforcing transmission lines and towers is a crucial measure to enhance power system resilience. Several existing studies have focused on transmission hardening planning (THP) prior to extreme weather events. Reference [4] developed a THP model based on distributionally robust optimization (DRO), using historical data to generate ambiguity sets of probability distributions. Reference [5] proposed a two-stage stochastic programming (SP) model for active distribution networks, obtaining coordinated planning strategies for line hardening and distributed energy resources. References [6] and [7] further incorporated the uncertainty of renewable energy output during extreme weather events. Building upon a two-stage robust optimization framework, they employed SP and DRO respectively to handle renewable generation uncertainties, resulting in more effective line hardening strategies.

As mentioned earlier, the widespread use of OPGW has tightly coupled transmission lines and communication links. Damage to OPGW caused by extreme weathers can lead to simultaneous interruptions in both power and information transmission. Therefore, it is essential to take into account the impacts of the cyber side when designing line hardening strategies. Reference [8] successfully incorporated cyber-physical coupling into THP, but its modeling was relatively oversimplified, leaving room for further research.

This paper proposes a transmission hardening planning methodology that considers cyber-physical coupling prior to extreme weather events. The main contributions are as follows:

1) A defender-attacker-defender (D-A-D) framework is established based on attack-defense game theory. The cyber-physical interactions in power CPS are modeled in the framework.

2) For the D-A-D model containing decision-dependent uncertainty (DDU), the special structure of the model is

This work was supported by National Natural Science Foundation of China (No. 52321004). (Corresponding author: Qinglai Guo).

XXX-X-XXXX-XXXX-X/XX/$XX.00 ©20XX IEEE
979-8-3315-8138-1

leveraged to eliminate the DDU and an efficient solution algorithm is designed based on column-and-constraint generation (C&CG).

## II. Transmission Hardening Planning Model

This section presents a transmission defense planning model based on the D-A-D framework. The strategy sets and objective functions of the outer-layer defender, the attacker, and the inner-layer defender are introduced in sequence.

### A. Outer-Layer Defender

First, the transmission lines are hardened prior to extreme weather events. The hardening decision variable of line $l$ is denoted as $x_l$, which is a binary variable (1: hardened, 0: unhardened). The overall objective function of the D-A-D framework is formulated as:

$$\min_{x} \sum_{l} c_l x_l + \max_{w,z,v \in U} Q(z,v) \tag{1}$$

where $c_l$ is the cost of hardening line $l$, and the max term represents the real-time dispatch cost under the worst-case extreme weather scenario.

The constraints in this layer include:

$$\sum_{l} r_l x_l \le R \tag{2}$$

where $r_l$ is the resource required to harden line $l$, and $R$ represents the total available resources for line hardening.

### B. Attacker

Following the hardening of transmission lines by the power system, extreme weather events attack the lines with the objective of maximizing the resulting real-time dispatch cost. The constraints in this layer include line attack constraints and nodal communication status constraints.

*1) Line attack constraints:*

The line attack constraints include:

*a) Attack permission constraint:*

$$k_{l,t} \le \eta_{l,t},\ \forall l, \forall t \tag{3}$$

where $k_{l,t}$ is a binary variable indicating the attack decision of extreme weather on line $l$ at time $t$ (1: attack, 0: no attack); $\eta_{l,t}$ is a parameter indicating whether extreme weather is permitted to attack line $l$ at time $t$ (1: permitted, 0: not permitted).

*b) Attack logical constraint:*

$$w_{l,t} = \sum_{\tau=1}^{t} k_{l,t},\ \forall l, \forall t \tag{4}$$

where $w_{l,t}$ is a binary variable indicating whether an extreme weather event has attacked line $l$ by time $t$ (1: attacked, 0: not attacked yet). This constraint ensures that each transmission line can be attacked at most once throughout the entire time horizon.

*c) Attack resource constraint:*

$$\sum_{l} w_{l,T} \le A \tag{5}$$

where parameter $A$ represents total attack resource, i.e. the maximum number of transmission lines that can be attacked by the extreme weather event. This constraint specifies that the total number of lines attacked throughout the entire time horizon must not exceed the total attack resource.

*d) Line status constraint:*

$$z_{l,t} = (x_l - 1) \cdot w_{l,t} + 1,\ \forall l, \forall t \tag{6}$$

where $z_{l,t}$ is a binary variable indicating the operational status of line $l$ at time $t$ (1: normal, 0: damaged). $z_{l,t} = 0$ if and only if $x_l = 0$ and $w_{l,t} = 1$, meaning that line $l$ is damaged only when it is unhardened and has been attacked by extreme weather by time $t$. Under all other conditions, the line remains in normal operation.

By adjusting the values of $\eta$ and $A$, the strategy set of extreme weather can be constrained, thereby regulating the robustness of the model-derived strategy and preventing overly conservative results.

*2) Nodal communication status constraints:*

In a power CPS, cyber-side failures primarily manifest as node communication failures. Normal nodal communication status requires two conditions: a functional power supply for the communication equipment, and the existence of a reachable routing path between the node and the control center. Currently, as most substation communication equipment in China utilizes redundant power supply configurations, the former condition is inherently satisfied and can be disregarded. For the latter one, a virtual flow method is introduced to determine the connectivity between each node and the control center in every time interval. The associated constraints include:

*a) Virtual flow injection constraint:*

$$0 \le u_{i,t} \le M \cdot S_{CC},\ \forall i, \forall t \tag{7}$$

where $u_{i,t}$ denotes the virtual flow injection decision variable at node $i$ and time $t$, $S_{CC}$ is a vector with a value of 1 only at the position corresponding to the control center and 0 elsewhere, and $M$ is a sufficiently large constant. This constraint restricts the virtual flow to be injected solely from the control center.

*b) Virtual flow outflow constraint:*

$$S_{CC} \le v_{i,t} \le 1,\ \forall i, \forall t \tag{8}$$

$$-(1 - z_{l,t}) \le v_{i,t} - v_{j,t} \le 1 - z_{l,t},\ \forall l = (i,j), \forall t \tag{9}$$

where $v_{i,t}$ represents the virtual flow outflow decision variable at node $i$ and time $t$, and also indicates its communication status. It is a binary variable (1: denotes normal communication, 0: communication loss).

Formula (8) ensures that the communication status of the control center remains normal, while formula (9) guarantees that two nodes connected by an operational line maintain identical communication status.

*c) Line virtual flow constraint:*

$$-M \cdot z_{l,t} \le F_{ij} \le M \cdot z_{l,t},\ \forall l = (i,j), \forall t \tag{10}$$

where $F_{ij}$ is the virtual flow amount on line $(i, j)$. This constraint ensures that no virtual flow is transmitted through damaged lines.

*d) Virtual flow balance constraint:*

$$u_{i,t} - v_{i,t} = \sum_{j \in i} F_{ij},\ \forall i, \forall t \tag{11}$$

This constraint ensures the conservation of virtual flow at each node.

Fig. 1 provides a simple illustrative example. The system comprises four nodes A, B, C, D in addition to the control center (CC). Solid lines represent normally operational transmission lines, while dashed lines denote damaged lines.

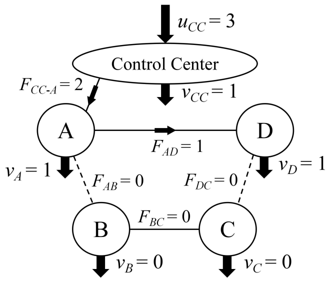


Fig. 1. A simple example for virtual flow method

For a given set of line status $z$, the existence of a reachable routing path between any node and the control center is deterministic. That is, the mapping from line status vector $z$ to the nodal communication state vector $v$ is a single-valued mapping. The aforementioned virtual flow method guarantees that for any arbitrary line state configuration $z$, there exists one and only one $v$ that satisfies constraints (7)-(11).

### C. Inner-Layer Defender

Following the attack on transmission lines by extreme weather events, the power system implements real-time dispatch, including the scheduling of generator outputs and the implementation of load shedding, to minimize overall losses. The objective function at this stage is formulated as:

$$Q(z,v)=\min_{p_{g,t},p_{w,t},\Delta p_{d,t}}\sum_t\sum_d c_d\Delta p_{d,t}+\sum_t\sum_g c_g p_{g,t}+\sum_t\sum_w c_w(P_{w,t}^{\max}-p_{w,t}) \tag{12}$$

where $\Delta p_{d,t}$, $p_{g,t}$, $p_{w,t}$ represent the load shedding at node $d$, the power output of thermal unit $g$, and the power output of wind farm $w$ at time $t$, respectively. The real-time dispatch cost expressed by the above equation comprises three components: load shedding cost, thermal generation cost, and wind power curtailment cost.

The constraints of this layer include:

*a) Thermal output constraint:*

$$v_{g,t}P_g^{\min}\le p_{g,t}\le v_{g,t}P_g^{\max},\ \forall g,\forall t \tag{13}$$

When the node hosting a thermal unit experiences communication loss, the unit becomes unmeasurable and uncontrollable. Protection system will subsequently trip the unit offline [9], resulting in $p_{g,t}=0$. This formulation approximates the physical state of a thermal unit following communication failure, modeling the impact of cyber-side anomalies on the physical system by constraining the unit's power output.

*b) Wind farm output constraint:*

$$0\le p_{w,t}\le v_{w,t}P_{w,t}^{\max},\ \forall w,\forall t \tag{14}$$

Similar to formula (13), when a wind farm experiences communication loss, its power output is also constrained to 0.

*c) Load shedding constraint:*

$$0\le\Delta p_{d,t}\le p_{d,t},\ \forall d,\forall t \tag{15}$$

*d) Power flow safety constraint:*

$$f_{l,t}=\frac{\theta_{i,t}-\theta_{j,t}}{X_l}\cdot z_{l,t},\ \forall l,\forall t \tag{16}$$

$$-F_l^{\max}z_{l,t}\le f_{l,t}\le F_l^{\max}z_{l,t},\ \forall l,\forall t \tag{17}$$

When a transmission line $l$ is in a damaged state at time $t$, i.e. $z_{l,t}=0$, the power flow $f_{l,t}$ on that line must be 0.

*e) Power flow safety constraint:*

$$\sum_{g\in G_i}p_{g,t}+\sum_{w\in W_i}p_{w,t}=\sum_{d\in D_i}(p_{d,t}-\Delta p_{d,t})+\sum_{l\in L_i}f_{l,t},\ \forall i,\forall t \tag{18}$$

## III. Solution Algorithm

This section designs a solution algorithm for the D-A-D model. First, the compact form of the model is derived. Then, the structure of the model is leveraged to eliminate the DDU. Finally, the C&CG algorithm is employed to solve the resulting optimization problem.

### A. Compact form

The D-A-D framework can be formulated into the following compact form:

$$\min_{x\in\mathbb{X}}a^{\mathrm T}x+\max_{w,z,v\in\mathbb{U}(x)}\min_{y\in\mathbb{Y}(z,v)}b^{\mathrm T}y \tag{19}$$

and

$$\mathbb{X}=\left\{x\,\middle|\,Ax\ge d,\ x\in\{0,1\}^{N_x}\right\} \tag{20}$$

$$\mathbb{U}(x)=\left\{w,z,v\,\middle|\,\begin{array}{c}Bw\ge e,\ w\in\{0,1\}^{N_w}\\ z=f(x,w)\\ v=g(z)\end{array}\right\} \tag{21}$$

$$\mathbb{Y}(z,v)=\left\{y\,\middle|\,Ey\ge h-Gz-Nv\right\} \tag{22}$$

where vector $x$ consists of the binary decision variables of the outer-layer defender; vectors $w$, $z$ and $v$ consist of variables of the attacker; vector $y$ consists of decision variables of the inner-layer defender; $f$ and $g$ are are single-valued mappings defined by formulas (6) and (7)-(11), respectively; $A$, $B$, $E$, $G$, $N$ are coefficient matrices and $a$, $b$, $d$, $e$, $h$ are coefficient vectors.

### B. Elimination of the DDU

Mathematically, this D-A-D framework shares the same formulation as an adaptive robust optimization (ARO) problem. Here, the uncertainty set $\mathbb{U}$ depends on the first-stage decisions $x$, exhibiting DDU. In general, ARO models with DDU cannot be solved using the C&CG algorithm directly and require further processing.

Note that within the DDU set $\mathbb{U}$, due to the fact that $f$ and $g$ are single-valued mappings, $z$ and $v$ are uniquely determined by $x$ and $w$, leaving only $w$ as a "free" variable. Consequently, moving the variables $z$ and $v$, along with their associated constraints, into the inner minimization problem does not compromise the equivalence of the original formulation. The model after transformation is formulated as:

$$\min_{x\in\mathbb{X}}a^{\mathrm T}x+\max_{w\in\mathbb{U}'}\min_{y,z,v\in\mathbb{Y}'(x,w)}b^{\mathrm T}y \tag{23}$$

and

$$\mathbb{X}=\left\{x\,\middle|\,Ax\ge d,\ x\in\{0,1\}^{N_x}\right\} \tag{24}$$

$$\mathbb{U}'=\left\{w\,\middle|\,Bw\ge e,\ w\in\{0,1\}^{N_w}\right\} \tag{25}$$

$$\mathbb{Y}'(x,w)=\left\{y,z,v\,\middle|\,\begin{array}{c}z=f(x,w)\\ v=g(z)\\ Ey+Gz+Nv\ge h\end{array}\right\} \tag{26}$$

The resulting model is free of DDU and can be solved using the C&CG algorithm.

### C. Applying C&CG Algorithm

The C&CG algorithm decomposes the original problem into a master problem (MP) and a subproblem (SP) [10]. The optimal solution is obtained by iteratively solving them until convergence.

The MP in the $n$-th iteration is formulated as:

$$\min_{x,\eta,y^k,z^k,v^k} a^{\mathrm{T}}x+\eta \tag{27}$$

s.t.

$$Ax \ge d,\ \ x\in\{0,1\}^{N_x} \tag{28}$$

$$\eta \ge b^{\mathrm{T}}y^k,\ \forall k\le n \tag{29}$$

$$z^k = f(x,w^{k*}),\ \ \forall k\le n \tag{30}$$

$$v^k = g(z^k),\ \ \forall k\le n \tag{31}$$

$$Ey^k+Gz^k+Nv^k \ge h,\ \ \forall k\le n \tag{32}$$

where $x$, $\eta$, $y^k$, $z^k$, $v^k$ are decision variables; $w^{k*}$ is the worst-case scenario identified by the SP in the ($k$-1)-th iteration. The MP is a mixed-integer linear programming (MILP) problem.

The SP in the $n$-th iteration is formulated as:

$$\max_{w\in\mathbb{U}'}\ \min_{y,z,v\in\mathbb{Y}'(\hat{x},w)} b^{\mathrm{T}}y \tag{33}$$

where $\hat{x}$ is the optimal solution of $x$ in the MP in the same round iteration.

By dualizing the inner minimization problem of (33), the SP can be transformed into a solvable form:

$$\max_{w,z,v,\lambda}(h-Gz-Nv)^{\mathrm{T}}\lambda \tag{34}$$

s.t.

$$E^{\mathrm{T}}\lambda = b \tag{35}$$

$$\lambda \ge 0 \tag{36}$$

$$Bw\ge e,\ \ w\in\{0,1\}^{N_w} \tag{37}$$

$$z = f(\hat{x},w) \tag{38}$$

$$v = g(z) \tag{39}$$

The products of binary variables $z$, $v$ and continuous dual variable $\lambda$ in the objective function (34) can be linearized using the big-M method. The SP after linearization is also an MILP problem.

## IV. Case Study

This section conducts case studies based on modified IEEE 30-bus and 118-bus systems. All computations are executed on a personal computer with an Intel Core Ultra 7 265K CPU (3.9 GHz) and 64 GB RAM, with code programmed by MATLAB and optimization problem solved by Gurobi 12.0.1.

### A. Modified IEEE 30-Bus System

#### 1) System settings:

The IEEE 30-bus system is modified as shown in Fig. 2. Two wind farms are added at buses 7 and 25. Buses connected by transformers are collectively treated as one communication substation, while other individual buses are each regarded as separate substations. The substation located at buses 6, 9 and 10 are designated as the control center. A simulated typhoon passes through this system, affecting a total of 12 transmission lines.

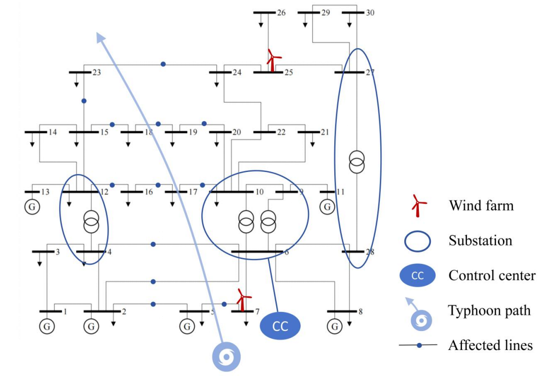


Fig. 2. Modified IEEE 30-bus system

#### 2) Algorithm performance and obtained strategy:

We set the total available hardening resources $R$=3 and total attack resource $A$=6. The algorithm converges in 11 iterations (390s). The upper bound (UB) and lower bound (LB) of the optimal objective value during iteration is illustrated in Fig. 3.

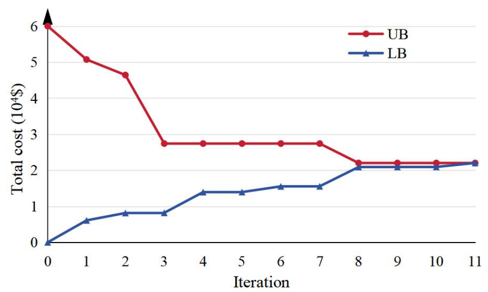


Fig. 3. UB and LB during iteration

In the obtained optimal hardening strategy, the lines selected for hardening are (4, 6), (5, 7) and (10, 17). Without line hardening, the worst-case scenario would involve the typhoon dividing the system into 3 isolated islands: the left section, the right section and bus 5, thereby causing communication loss in the left section and bus 5. In the optimal hardening strategy, lines (4, 6) and (5, 7) are protected. This effectively prevents the aforementioned worst-case scenario, demonstrating the efficacy of the obtained strategy.

#### 3) Comparison analysis:

To validate the effectiveness of the proposed model, the hardening strategy obtained from our model are compared with those derived from (a) D-A-D model that ignores cyber-physical coupling, and (b) SP model that considers cyber-physical coupling. Based on formula (3), 200 test samples of line damage are generated via Monte Carlo simulation.

The optimal hardening strategy derived from D-A-D model that ignores cyber-physical coupling with $R$=3 and $A$=6 is (12, 16), (16, 17) and (19, 20). The costs of the two strategies across all test samples are shown in Fig. 4.

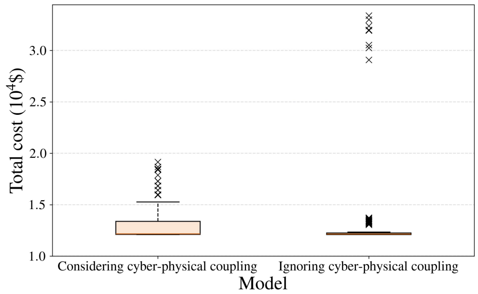


Fig. 4. Results comparison of considering cyber-physical coupling and not

When a cyber-physical coupling-integrated line hardening strategy is adopted, no generator buses experience communication loss across all test scenarios. In contrast, if cyber-physical coupling is ignored, generator bus disconnections occur in 8 scenarios (4.0%), leading to insufficient generation capacity and substantial load shedding. These results demonstrate the necessity of considering cyber-physical coupling in the THP problem.

We develop an SP model that incorporates cyber-physical coupling based on the sample average approximation (SAA) method. By randomly sampling 200 line damage scenarios, the model aims to minimize the average cost across all sampled scenarios.

The strategy obtained from the SP model is to harden none of the transmission lines. The costs of the two strategies derived from the D-A-D model and the SP model across all test samples are shown in Fig. 5.

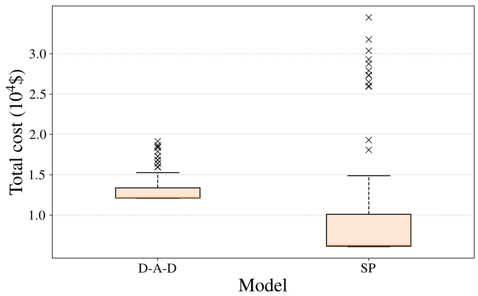


Fig. 5. Results comparison of D-A-D and SP model

If the strategy obtained from the SP model is implemented, generator bus disconnections would occur in 13 scenarios (6.5%). Therefore, the proposed D-A-D model exhibits stronger robustness, and the resulting strategy better meets the requirements for enhancing power CPS resilience.

### *B. Modified IEEE 118-Bus System*

In the modified IEEE 118-bus system, 6 wind farms are added at buses 12, 26, 46, 54, 66 and 100. The control center is located at bus 49. A simulated typhoon passes through this system, affecting a total of 13 transmission lines. The modified system is shown in Fig. 6.

We set the total available hardening resources $R$=3 and total attack resource $A$=6. The algorithm converges in 15 iterations (760s), demonstrating its computational efficiency even for large-scale systems. The obtained optimal hardening strategy is (23, 24), (30, 38) and (37, 38).

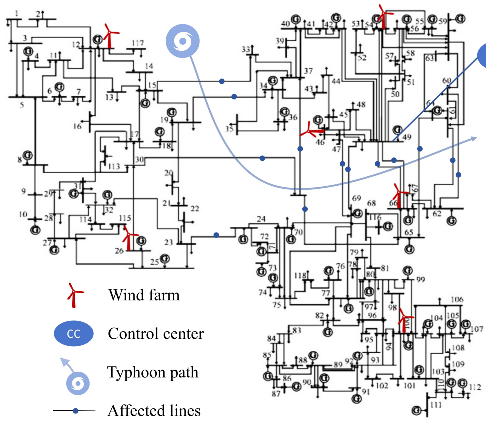


Fig. 6. Modified IEEE 118-bus system

## V. CONCLUSION

To enhance power CPS resilience against extreme weather, this paper proposes a THP method that considers cyber-physical coupling. A D-A-D framework is established where cyber-physical interactions are explicitly modeled. The special structure of the model is leveraged to eliminate the DDU, then the C&CG algorithm is applied. Case studies demonstrate the necessity of incorporating cyber-physical coupling in THP, and the proposed model and algorithm exhibit strong applicability on both the 30-bus and 118-bus systems. Future research directions include improving the accuracy of cyber-physical interaction modeling and incorporating the impacts of renewable energy uncertainty.

## REFERENCES

[1] H. Sun, Q. Guo, X. Shen, Y. Xue, M. Shahidehpour, and N. Hatziargyriou, "Energy Internet: Redefinition and Categories," *Energy Internet*, vol. 1, no. 1, pp. 4-8, 2024.

[2] S. V. Buldyrev, R. Parshani, G. Paul, H. E. Stanley, and S. Havlin, "Catastrophic Cascade of Failures in Interdependent Networks," *Nature*, vol. 464, no. 7291, pp. 1025-1028, 2010.

[3] F. H. Jufri, V. Widiputra, J. Jung, "State-of-the-Art Review on Power Grid Resilience to Extreme Weather Events: Definitions, Frameworks, Quantitative Assessment Methodologies, and Enhancement Strategies," *Appl. Energy*, no. 239, pp. 1049-1065, 2019.

[4] J. Yan, B. Hu, K. Xie, J. Tang and H. -M. Tai, "Data-Driven Transmission Defense Planning Against Extreme Weather Events," *IEEE Trans. Smart Grid*, vol. 11, no. 3, pp. 2257-2270, 2020.

[5] A. Poudyal, S. Poudel and A. Dubey, "Risk-Based Active Distribution System Planning for Resilience Against Extreme Weather Events," *IEEE Trans. Sustain. Energy*, vol. 14, no. 2, pp. 1178-1192, 2023.

[6] X. Wang, Z. Li, M. Shahidehpour and C. Jiang, "Robust Line Hardening Strategies for Improving the Resilience of Distribution Systems With Variable Renewable Resources," *IEEE Trans. Sustain. Energ*, vol. 10, no. 1, pp. 386-395, 2019.

[7] A. Bagheri, C. Zhao, F. Qiu and J. Wang, "Resilient Transmission Hardening Planning in a High Renewable Penetration Era," *IEEE Trans. Power Syst.*, vol. 34, no. 2, pp. 873-882, 2019.

[8] X Li, W Li, N Wang, L Li and X Gong, "Resilience Enhancement by Line Hardening for Communication Routing Considering Renewable Energy Sources in Cyber-Physical Power Systems," *IET Renew. Power Gener.*, vol. 18, no. 14, pp. 2477-2495, 2024.

[9] G. Huang, J. Wang, C. Chen and C. Guo, "Cyber-Constrained Optimal Power Flow Model for Smart Grid Resilience Enhancement," *IEEE Trans. Smart Grid*, vol. 10, no. 5, pp. 5547-5555, 2019.

[10] B. Zeng and L. Zhao, "Solving Two-Stage Robust Optimization Problems Using a Column-and-Constraint Generation Method," *Oper. Res. Lett.*, vol. 41, no. 5, pp. 457-461, 2013.

979-8-3315-8138-1